

# Optimization and Validation of Microstrip Patch Antenna for Endoscopy Application

Juily Nachiket Tarade<sup>1</sup> <sup>a</sup> and Uday Pandit Khot<sup>2</sup>

<sup>1</sup>Electronics and Telecommunication Engineering Department, Ramrao Adik Institute of Technology, Nerul, Navi Mumbai, Mumbai University, Maharashtra, India

<sup>2</sup>Electronics and Telecommunication Engineering Department, St. Francis Institute of Technology, Borivali, Mumbai University, Maharashtra Maharashtra, India


**Keywords:** Microstrip Patch Antenna, Electromagnetic Bandgap, Non-Invasive, Specific Absorption Rate, Wireless Capsule Endoscopy, Link Budget.

**Abstract:** Compared to standard endoscopy, wireless capsule endoscopy with non-invasive antennas has gained more attention. Since the transmitting antenna of a wireless capsule endoscope (WCE) is located inside the body as opposed to the receiving antenna, which is located outside of it, designing the transmitting antenna is a difficult challenge. Simultaneously achieving high data rates, small size, omni-directionality, acceptable specific absorption rate (SAR), and large bandwidth in telemetry systems are major hurdles faced by these antennas. This is because many parts of the gastrointestinal tract have different dielectric constants and thicknesses. To overcome these obstacles, antennas must be characterized for WCE. With a modified partial ground plane, the suggested antenna is a small planar slotted microstrip patch antenna. It is a miniature ingestion-capable Ultra-Wide Band (UWB) antenna. The substrate material for the antenna is Rogers TMM 13i. An environment that roughly represents the full human gastrointestinal (GI) tract, including surrounding tissues is created using the High Frequency Structure Simulator (HFSS 13.0). The performance of the antenna is evaluated by placing it in the middle of the various GI tracts. The suggested antenna's dimensions are 40 mm<sup>3</sup> (10 mm × 10 mm × 0.4 mm) and is a mere 1.26 percent of the capsule's volume. About 4.3 GHz and 6.7 GHz, with a -3 dB bandwidth of about 20.4 MHz and 950 MHz, respectively, are the resonant frequencies. The advantage of having multiple resonant frequencies is that the proposed single antenna can be used for all the GI tract although the dielectric constant varies over the entire GI tract. The existing literature needs different antennas for different GI tracts. In the biological model, the radiation pattern is circularly polarized and omnidirectional. The maximum radiation efficiency of 95.65% has been observed. For the purpose of biocompatibility analysis, the SAR value in the GI tract is also calculated and is in well limit. Once patch is designed for endoscopy application, it needs to be validated which can be done with the help of link budget where  $A_p > R_p$ . To establish a stable communication link between the endoscopic antenna and external device, the antenna power ( $A_p$ ) should be higher than the required power ( $R_p$ ).

## 1 INTRODUCTION

Today's cutting-edge wireless capsule endoscopy technology replaces the conventional endoscopy method, which uses a wired endoscope to diagnose the digestive tract. Due to the fact that endoscopy can only access the duodenum, which is the upper portion of the small intestine, because of its horrible consequences, particularly in younger aged individuals and children (Mulugu and Saha , 2020).

A contemporary non-invasive method for diagnosing life-threatening conditions including inflammatory small intestinal diseases like Crohn's disease is called wireless capsule endoscopy. Cancer, colon polyps, tumours, and gastrointestinal bleeding in the digestive tract that, if discovered at preliminary phases (Mulugu and Saha , 2020). Therefore, this diagnosing method which has gained attention recently is of the utmost relevance. The antenna, which transfers image data from the sophisticated CMOS image sensor in the capsule to the on-body

<sup>a</sup> <https://orcid.org/0009-0008-2851-5707>

receiver antennas, is a crucial part of the wireless capsule endoscopy system. The challenge of designing a miniaturised antenna that can fit into a capsule of this size and still leave room for other essential components like LEDs, a CMOS imager, an antenna, a battery, and other electronics arises from the capsule's size restrictions due to the narrow passageways of the digestive system (Mulugu and Saha, 2020). An antenna with an omnidirectional radiation pattern is necessary due to the capsule's uncontrollably orientated orientation. Another design problem to satisfy high data rate needs for transmitting high-resolution images at fast frame rates is wide bandwidth. Furthermore, the antenna's broad bandwidth lessens the impact of significant frequency fluctuations on its performance, allowing it to endure the fluctuating conditions of the digestive system (Sarestoniemi, et al., 2020). Recent history reports a great deal of research and advancement in this field.

A compact planar slotted microstrip patch antenna with a modified partial ground plane and resonance frequencies of around 4.3 and 6.6 GHz is the proposed antenna in this research. The design of this structure at UWB frequency offers a significant deal of opportunity for increasing bandwidth and utilizing UWB technology's low power and high penetration capabilities, among other benefits. The size of the proposed antenna is  $90 \text{ mm}^3$  ( $10 \text{ mm} \times 10 \text{ mm} \times 0.9 \text{ mm}$ ) which is only 1.26% of the capsule volume. Normally the capsule is of ( $26 \times 11 \text{ mm}^2$ ). The radiation pattern is omnidirectional with circular polarization in the biological model. It is observed that the maximum radiation efficiency is 95.65%. The EBG structure is optimized using the Particle Swarm Optimization (PSO) method in order to reduce SAR. There is significant reduction in SAR values at every stage of GI track. SAR values significantly decrease over the whole GI track. The EBG structure causes a little drop in gain (15.65% decrease in antenna gain in the esophagus at 6.7 GHz as compared to the absence of EBG), but this has no effect on the gearbox because the radiated power (2.89 mW) and radiation efficiency (typically ranges between 40% and 70%) are within an acceptable range. The acceptable range of radiated power is 3.1 mW and radiation efficiency (typically ranges between 40% and 70%) for endoscopy application. There is little impact on the fractional BW. The entire simulations are performed in HFSS 13.0. The antenna design, simulation setup, results, link budget and conclusions are organized into sections 2, 3, 4, 5 and 6 respectively.

## 2 DESIGN OF MICROSTRIP PATCH ANTENNA FOR ENDOSCOPY APPLICATION

The proposed UWB compact planar slotted patch antenna is designed on a Rogers TMM 13i substrate with a high relative permittivity, allowing for a reduction in effective wavelength. Table 1 summarizes the dimensions of the proposed antenna. The antenna's radiation properties are enhanced by using the partial ground plane, with the upper corners of the ground deleted and notches added to improve bandwidth and impedance matching. A plus (+) form slot is added in the middle of the patch, and a split ring slot is placed around the slot to maximize resonance frequency and improve bandwidth. Two square slots are added to create a single feed, circularly polarized antenna. Human models of the stomach, esophagus, small intestine, and large intestine are built for simulation to study anatomical factors affecting the effectiveness of the transmitting antenna. The antenna provides circular polarization and an omnidirectional emission pattern, with a -3 dB fractional bandwidth of 1.16% and 9.55% respectively. Paper (Tarade and Khot, 2024) addressed the design, simulation, and analysis of a miniature UWB ingestible capsule antenna for wireless capsule endoscopy. For better transmission, radiation efficiency need to be improved while antenna travels through small and large intestine. SAR need to be reduce.

Table 1: Dimensions of Proposed Antenna (Wang, et al., 2018)

Parameters	Values (mm)
Substrate	length = 10, Width ( $W$ ) = 10, Thickness = 0.4,
Patch	$C1 = 2.5$ ; $C2 = 1.5$ ; $C3 = 1.3$ , $S1 = 1$ ; $S2 = 0.5$ ; Thickness = 0.25
Feed line	Thickness = 0.25, $M = 3.2$ , $F1 = 1.8$ ; $F2 = 1.8$
Ground	Thickness = 0.25, $A = 3$ ; $B = 1$ ; $C = 2.8283$

### 2.1 Reduction of SAR using Optimized EBG Structure

The Specific Absorption Rate (SAR) is a crucial aspect of antenna design, particularly for portable communication systems. It is determined by the Institute of Electrical and Electronics Engineers (IEEE) and the International Commission on Non-Ionizing Radiation Protection (ICNIRP) (Mously, et

al. , 2011). The EBG structure is a man-made periodic structure that helps electromagnetic waves propagate or divert due to the periodic variation in the refractive index inside it. The EBG method is preferred for SAR reduction due to its wide range of resonant and cross polarization effects (Bhavarthe, Rathod , et al. , 2018).

The EBG structure is optimized using the Particle Swarm Optimization (PSO) method, which tracks a swarm of particles representing potential resolutions. The dispersion analysis is the first step in designing an EBG structure, with unit cell modeling and application of periodic boundary conditions in the appropriate directions as the foundation. The fitness function  $F$  is formulated as a two-criterion function, which is shown in equation (1) and a minimization of the function is planned (Dutta, Jayasree , et al. , 2016).

$$F = \left[ \frac{f_{\max} + f_{\min}}{2} - f_c \right] - \left[ \frac{f_{\max} - f_{\min}}{f_c} \right] \quad (1)$$

$$\text{Where } f_{\min} = \frac{\omega_0}{2\pi} + \frac{1}{2\pi\eta_0 C} \quad (2)$$

$$f_{\max} = \frac{\omega}{\pi} - f_{\min} \quad (3)$$

Where  $f_{\min}$  is the lower limit and  $f_{\max}$  is the upper limit of the band gap, which is shown in the equation (2) and (3). This fitness function has been used in PSO for optimizing the EBG structure. The PSO algorithm has been tested on a simple planar EBG unit cell depicted in Figure 1. The square patch size  $P$  and the period  $D$  were chosen as the state variables for the optimization (Dutta, Jayasree , et al. , 2016).

The best approach is to use RF-Shields, particularly when using the EBG substrate. However, care must be taken to preserve other crucial elements impacting the antenna's performance, such as impedance matching, which offers high efficiency, shrinks the antenna's size, increases its compactness and robustness, and integrates with existing RF circuit component.

## 2.2 Simulation Results

The proposed antenna with EBG Structure is shown in the Figure 2 (a) The antenna is placed at the center of the esophagus tissue models of the GI tract, as shown in Figure 2 (b) and corresponding simulations are carried out to by using HFSS ver. 13.0.

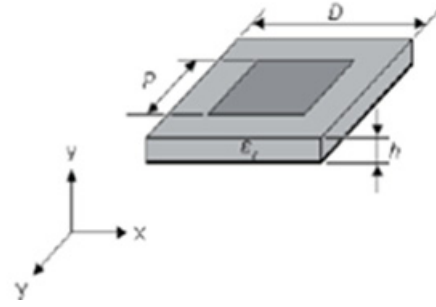


Figure 1: EBG cell under consideration (Kennedy and Eberhart , 1995)

### 2.2.1 S- Parameter and Bandwidth

The reflection coefficient ( $|S_{11}|$ ) of the ingestible capsule antenna at the center of the esophagus tissue models of GI tract are exhibited in Figure 3.

The antenna resonates at 3.62 GHz and 4.84 GHz inside the esophagus, with a reflection coefficient of -11.01 dB and -13.52 dB respectively.

### 2.2.2 Radiation Pattern

The 2D far field radiation pattern of the antenna in E-plane and H-plane inside the oesophagus tissue models at the resonant frequencies 3.62 GHz and 4.84 GHz are shown in the Figure 4 (a), (b) and Figure 5 (a), (b) respectively. It exhibits an omni-directional radiation pattern, transmitting information in all directions. From the radiation pattern, it is obvious that the antenna exhibits omni-directional radiation pattern throughout the oesophagus. So the antenna will be able to transmit information in all directions independent of the direction and orientation of the capsule which is essential for ingestible antenna.

3-D polar plot inside esophagus tissue model for proposed antenna with EBG is shown in the Figure 6. Maximum gain is about -28 dB at 4.3 GHz and -29.60 dB at 6.6 GHz.

### 2.2.3 Specific Absorption Rate (SAR)

The simulated distributions of local SAR averaged over 10 g tissue when the capsule antenna with EBG is placed inside esophagus models are shown in the Figure 7 (a) and (b). IEEE C95.1- 2005 standard limits 10g-avg SAR is 2 W/Kg and the IEEE C95.1-1999 standard limits 1g-avg SAR is 1.6 W/Kg. The maximum SAR is calculated for input power of 1W through the esophagus averaged over 10g of tissue is 0.127 W/kg at 4.3 GHz and 1.17 at 6.6 GHz. In order to keep match with IEEE C95.1-2005 standard, the maximum allowable net input power for the proposed

design of capsule antenna at 3.62 GHz is 854.3 mW and 736.7 mW at 4.84 GHz. Since Rogers TMM 13i is a ceramic thermoset polymer composite (Rogerscorp.com, et al., 2018), it might be harmless to the GI tract in case of unexpected disruption of the capsule.

In summary, achieving a low SAR is essential for various antenna applications, including wearable or mobile phone antennas. The EBG structure is a significant design that can enhance antenna performance without sacrificing bandwidth.

### 3 OPTIMIZED MICROSTRIP PATCH ANTENNA DESIGN

All performance and safety measures of the ingestible antenna (without EBG) for four different tissue models of GI tract (esophagus, stomach, small intestine, and large intestine for two resonant frequencies are exhibited in Table 2 and all the performance measures of the ingestible antenna (with EBG) shown in the Table 3.

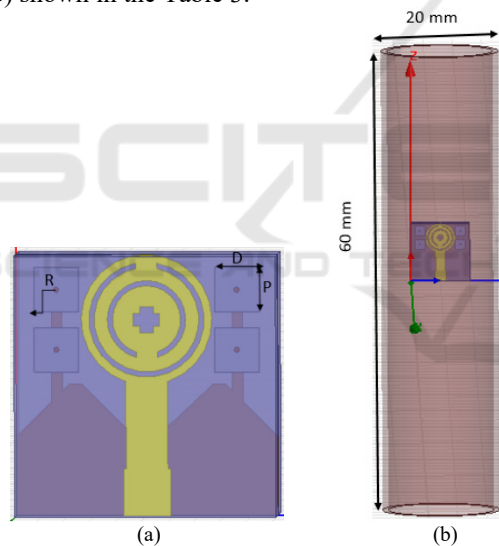


Figure 2: Proposed antenna with (a) EBG Structure (b) antenna with EBG Structure place in Esophagus tissue model.

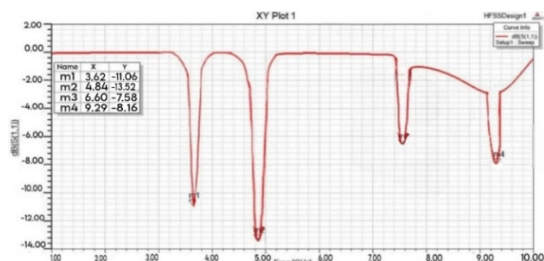
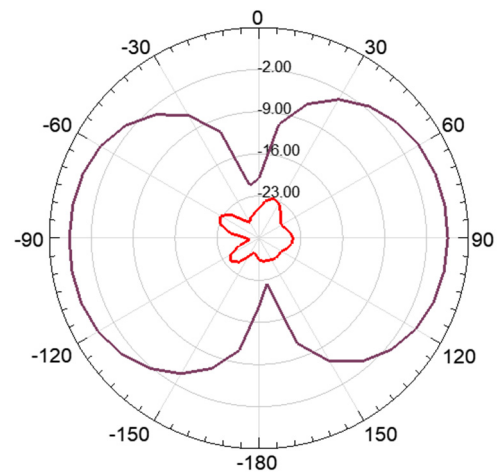
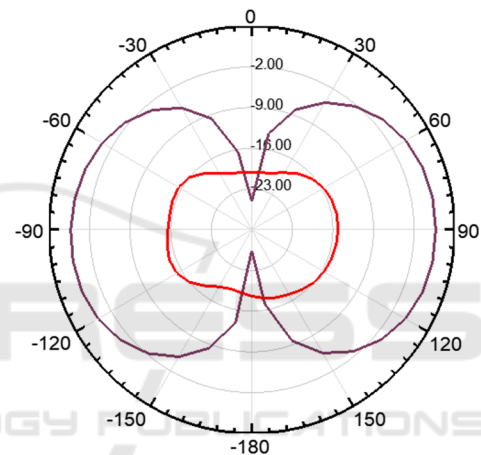


Figure 3: Reflection coefficient frequency responses of the antenna with EBG in esophagus model.

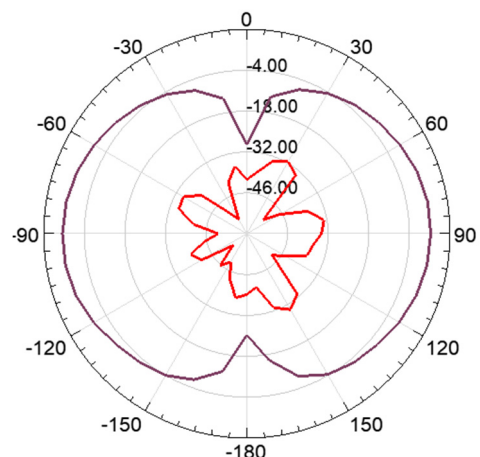


(a)



(b)

Figure 4: Far-field directivity radiation pattern of the antenna with EBG at 3.62 GHz through the esophagus tissue model (a) E – Plane (b) H – Plane



(a)



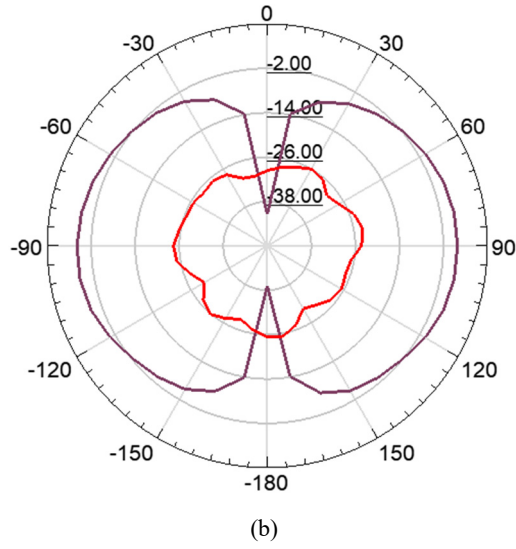


Figure 5: Far-field directivity radiation pattern of the antenna with EBG at 4.84 GHz through the esophagus tissue model (a) E – Plane (b) H – Plane

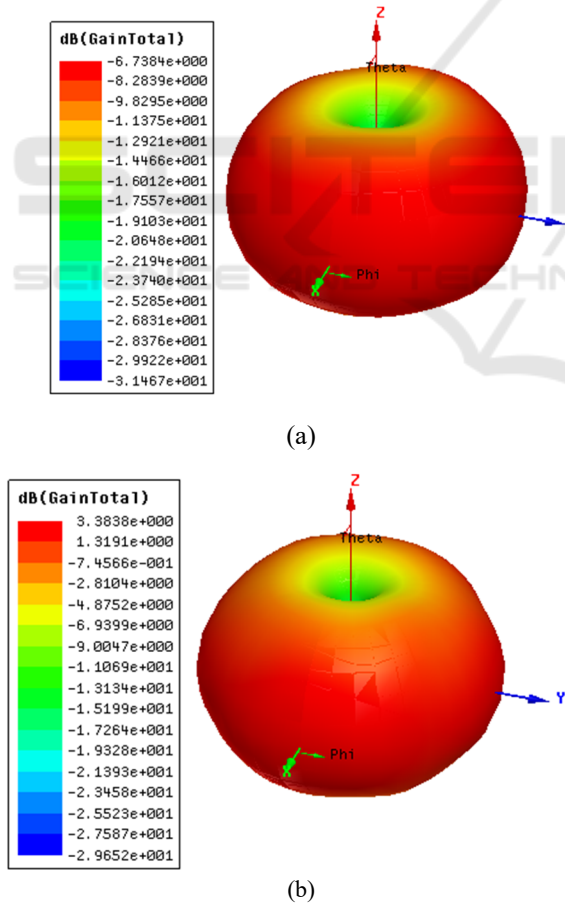


Figure 6: 3-D polar plot of proposed antenna with EBG at (a) 3.62 GHz and (b) 4.84 GHz

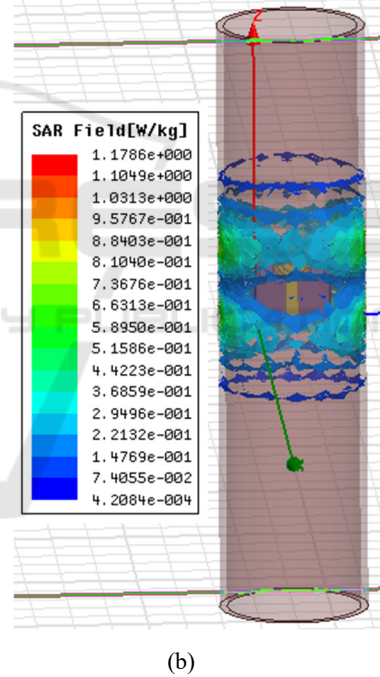
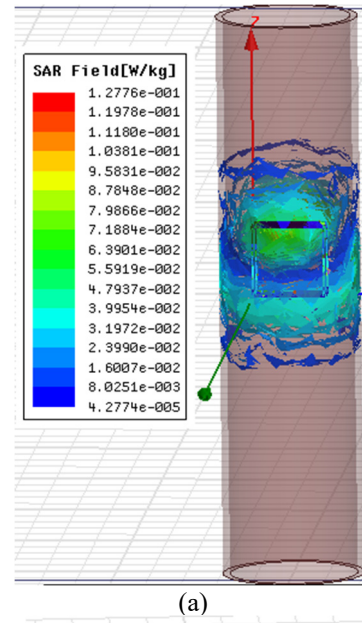


Figure 7: Simulated distributions of local SAR averaged over 1 g tissue for esophagus model at resonant frequency (a) 3.62 GHz (b) 4.84 GHz

Table 4 shows comparison of SAR reduction by using EBG Method. There is significant reduction in SAR values at every stage of GI track. Although because of the EBG structure there is a slight reduction in gain, the radiated power and hence radiation efficiency is in acceptable range which will not affect the transmission. The fractional BW is not getting affected much.

#### 4 VALIDATION USING LINK BUDGET

Using implanted transducers, a biomedical telemetric link enables remote physiological assessments. Consequently, a trustworthy channel of communication is necessary between the patient's external controlling and/or monitoring equipment and the in-body device. However, a number of losses, including route loss, reflection, absorption (Zada and Yoo, 2018), and polarisation mismatch losses (Shah and Yoo, 2018), make it difficult to guarantee the communication link's robustness. We attributed the highest value of polarisation losses in our connection analysis to the use of a linearly polarised antenna, which is capable of changing orientation as it passes through the GI tract. Additionally, implantable devices have limited input power and effective isotropic radiated power (EIRP) to prevent safety concerns and interference with adjacent devices using the same frequencies. As a result, for the 402 MHz and 915 MHz bands, respectively, the EIRP must be less than or equal to the  $EIRP_{max} = -16$  dBm and 36 dBm. Compared to higher frequencies, the signal travels through the body more consistently at lower

frequencies. Therefore, deep skin implantations and GI applications are better suited for lower frequencies. Endoscopic devices may have additional power limitations due to their electronic circuitry and batteries than EIRPs (Faisal and Yoo, 2019). The devices of the endoscopic capsule type employ 20 mW silver oxide batteries, which can constantly supply the circuit with 3V at 55 mAh for 8–10 hours. The transmitter power ( $P_t$ ), which is less than the maximum permitted input power (determined using the maximum SAR values), is kept at -4 dBm in consideration of these difficulties. Because high data rates are necessary for capsule endoscopy in order to transport high-quality images to the external base station, the value of  $B_r$  is taken to be 1 Mb/s. In order for the endoscopic antenna and external device to create a reliable communication link, the antenna power ( $A_p$ ) must be greater than the needed power ( $R_p$ ). The following is a method for calculating  $A_p$  and  $R_p$  values:

$$A_p \text{ (dB)} = P_{Tx} + G_{Tx} + G_{Rx} - L_f - P_L, \quad (4)$$

$$R_p \text{ (dB)} = E_b/N_o + K T_o + B_r, \quad (5)$$

Table 2: Antenna Parameters in Different Tissues at Different frequencies (Without EBG) (1 Watt I/p Power)

Parameters	Esophagus		Stomach		Small Intestine		Large Intestine	
	4.3 GHz	6.6 GHz	4.3 GHz	6.6 GHz	4.3 GHz	6.6 GHz	4.3 GHz	6.6 GHz
S11 dB	-10.76	-15.34	-9.239	-23.55	-6.102	-4.459	-7.17	-5.077
BW <sub>3dB</sub> (MHz)	170	760	160	930	140	340	150	390
Fractional BW (%)	3.96	11.51	3.71	14.13	3.24	5.11	3.48	5.90
Radiation Efficiency (dB)	6.38	95.65	5.40	96.09	1.27	35.18	5.10	61.43
Maximum Gain (dB)	-13.75	-18	-12.25	-22.15	16.60	-22.25	-11.70	-11.25
Max. SAR [W/kg]	0.079	40.8	0.0045	7.54	1.368	1050	234	208
Radiated power (Mw)	0.430	276.4	0.372	372.01	$9.483 \times 10^{-5}$	234.05	0.388	79.75
Accepted Power (Mw)	6.738	288.99	6.884	387.12	7.41	665.21	7.60	129.81
Peak Gain(dBi)	0.108	1.6035	0.0688	1.6794	0.0309	0.6130	0.1389	1.1951
Front to back ratio	2.385	1.068	1.2529	1.1004	1.4126	1.7683	2.3193	1.4425
Peak Directivity	1.702	1.6764	1.274	1.7476	2.4188	1.7425	2.7225	1.9452

Table 3: Antenna Parameters in Different Tissues at Different Frequencies (With EBG) (1Watt I/p Power)

Parameters	Esophagus		Stomach		Small Intestine		Large Intestine	
$f_r$ (GHz)	3.62	4.84	3.62	4.84	3.62	4.84	3.62	4.84
S11  (dB)	-3	-3.1	-10	-11.06	-8.06	-8.09	-8.5	-7.01
BW <sub>3dB</sub> (MHz)	700	420	370	360	360	340	370	410
Fractional BW (%)	10.66	9.37	9.67	8.12	7.89	9.89	7.23	8.23
Radiation Efficiency (%)	12.3	93.12	2.40	26	2.38	26	12.15	22.95
Maximum Gain (dB)	-28	-29.60	-26.75	-30.30	26.70	-30.30	-27.75	30.25
Max. SAR [W/kg]	0.127	1.78	0.0045	7.45	1.368	2.45	1.06	57.22
Radiated power (mW)	1.798	24.52	0.325	2.89	0.324	2.89	1.76	2.78
Accepted Power (mW)	14.56	26.33	13.5	11.14	13.7	11.14	14.5	12.14
Peak Gain (dBi)	0.211	2.18	0.042	0.68	0.043	0.68	0.20	0.61
Front to back ratio	1.065	1.03	2.56	1.11	2.55	1.11	1.13	1.15
Peak Directivity	1.72	2.34	1.77	2.62	1.81	2.62	1.69	2.66

Table 4: Comparison of SAR reduction by using EBG Method

Parameters	Esophagus		Stomach		Small Intestine		Large Intestine	
$f_r$ (GHz)	4.3	6.6	4.3	6.6	4.3	6.6	4.3	6.6
Max. SAR [W/kg] Without EBG	0.145	1.17	38.45	59.47	41.34	1050	234	208
Max. SAR [W/kg] With EBG	0.127	0.198	0.0045	7.54	1.368	25.45	1.06	51.22
Reduction in SAR %	13.79	83.07	99.98	87.32	96.69	97.57	99.54	75.37

where  $G_{Rx}$ ,  $G_{Tx}$ , and  $P_{Tx}$  stand for the receiver antenna's gain, transmitter power, and transmitter gain, respectively. Receiving antenna is placed on body near esophagus (approximately 5 cm distance from transmitting antenna) which is moving through GI tract. As the transmitting antenna moves through stomach, small intestine, large intestine the distance increases. Figure 8 shows the plotted connection margins for the stomach, large intestine, and small intestine. Table 5 shows that the value of  $G_{Tx}$  varies depending to the implantation scenario, whereas the value of  $G_{Rx}$  is thought to be constant at 0.042 dBi. The free space and polarisation mismatch losses are represented by  $L_f$  and  $P_L$ , respectively. In general, the distance ( $d$ ) between the transmitter and the receiver determines  $L_f$ . The following formulas can be used to calculate this loss:

$$L_f \text{ (dB)} = 20 \log (4\pi d / \lambda) \quad (6)$$

In equation (5), the optimal phase shift keying, temperature, Boltzmann constant, and data rate are denoted by  $E_b/N_0$ ,  $K$ ,  $T_0$ , and  $B_r$ , respectively.

Table 5: Key factors taken into account for link budget analysis.

Parameters	Value
Resonance frequency $f_0$ (GHz)	3.62/4.84
Noise power density $N_0$ (dB/Hz)	-203.93
Transmitter power $P_{Tx}$ (dBm)	-4.33
Polarization mismatch loss $P_L$ (dB)	1
Temperature $T_0$ (Kelvin)	273
Free space path loss $L_f$ (dB)	Distance dependent
Transmitter antenna gain $G_{Tx}$ (dBi)	Scenario dependent
Receiver antenna gain $G_{Rx}$ (dBi)	0.042
Boltzmann Constant $K$	$1.38 \times 10^{-23}$
Available power $A_P$ (dB)	Distance dependent
Bit rate $B_r$ (Mbps)	1
Required power $R_P$ (dB)	-134.64
Margin $A_P - R_P$ (dB)	Fig. 8

Table 5 contains a list of all the previously discussed parameters together with their values used to calculate the connection. The suggested endoscopic antenna has been shown to reliably transmit data across a distance of over 25 cm at 20 dB margins for both frequencies in a variety of implanted circumstances.

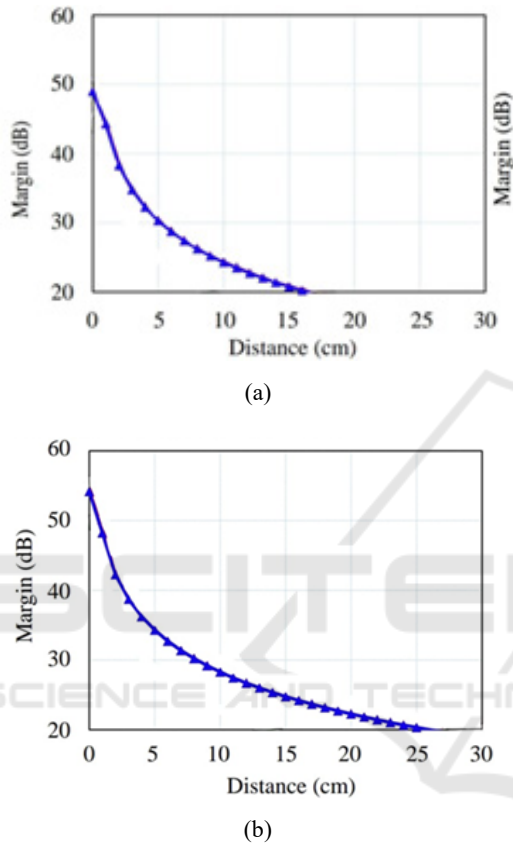


Figure 8: Link budget analysis at 1 Mbps in different implanted organs (a) 3.62 GHz (b) 4.84 GHz.

## 5 CONCLUSIONS

The Specific Absorption Rate (SAR) is the most important factor to consider. Because the absorption of harmful electromagnetic waves can cause serious injury to the human body. Especially when designing antennas for wearable technology or cell phones that come into direct touch with the human body. It is possible to reduce the SAR value by adjusting a number of parameters, such as antenna position, size, and thickness. The EBG substrate is the most effective method. But when using this method to reduce the SAR value, it's important to keep in mind other important factors that affect the antenna's performance, like impedance matching, which

provides high efficiency, reduces the size of the antenna, makes it more compact and robust, and integrates with the existing RF circuit components.

The proposed antenna is only 1.26 percent of the capsule's volume, measuring 40 mm<sup>3</sup> (10 mm × 10 mm × 0.4 mm). The resonant frequencies are around 4.3 GHz and 6.7 GHz, with a -3 dB bandwidth of roughly 20.4 MHz and 950 MHz, respectively. Having numerous resonant frequencies has the benefit of allowing the proposed single antenna to cover the whole GI system, even if the dielectric constant changes throughout the GI tract. Different antennas are required for various GI tracts in the literature currently under publication. The radiation pattern is omnidirectional and circularly polarized in the biological model. The highest recorded radiation efficiency was 95.65%. Additionally computed for the purpose of biocompatibility analysis, the GI tract's SAR value is within the well limit. PSO aids in lowering the SAR by optimizing the EBG structure's dimensions. Table VI shows a considerable drop in SAR values at each level of the GI track. The gearbox won't be impacted by the EBG structure's little reduction in gain because the radiated power and, consequently, radiation efficiency, are within a reasonable range. The fractional BW is not much affected. The link budget and SAR analysis were conducted to ensure the reliability of the wireless link and user safety, respectively.

## 6 FUTUTRE SCOPE

Additional body parameters may be included in channel modelling of communication for more accuracy purpose.

## REFERENCES

- R. Mulugu, and C. Saha, "Design, Development and Realization of UWB Antenna for Wireless Capsule Endoscopy," *In IEEE Int. Symp. on Antennas & Propag. (APSYM)*, pp.19-21, Dec. 2020.
- M. Sarestoniemi *et al.*, "WBAN channel characteristics between capsule endoscope and receiving directive UWB on-body antennas," *IEEE access*, vol. 8, pp.55953-55968, Mar. 2020.
- J. Wang *et al.*, "An Implantable and Conformal Antenna for Wireless Capsule Endoscopy" *IEEE Antennas and Wireless Propag. Lett.*, vol. 17, no. 7, pp. 1154-1157, May 2018.
- J. Tarade and U. P. Khot, "Characterization of Microstrip Patch Antenna for Endoscopy Application" *Int. J. of*



- Electronics and Communication Engineering (IJECE)*, vol. 11(8), pp. 207-217, August 2024.
- S. I. Al-Mously, "Factors influencing the EM interaction between mobile phone antennas and human head," In *Int. Conf. on Digital Information and Communication Technology and Its Applications*, 2011, pp. 106-120.
- P. P. Bhavarthe, S. S. Rathod, and K. Reddy, "A compact dual band gap electromagnetic band gap structure," *IEEE Trans. on Antennas and Propagation*, vol. 67, pp. 596- 600, 2018.
- P. K. Dutta, P. V. Y. Jayasree, and V. S. S. N. S. Baba, "SAR reduction in the modelled human head for the mobile phone using different material shields," *Human-centric Computing and Information Sciences*, vol. 6, pp. 1-22, 2016.
- J. Kennedy, and R. Eberhart, "Particle swarm optimization," In *Proc. of ICNN'95- IEEE int. conference on neural networks*, vol. 4, pp. 1942-1948, Nov. 1995.
- Rogerscorp.com, 'TMM® 13i Laminates', 2018 [online]. Available:  
<https://www.rogerscorp.com/acs/products/51/TMM-13iLaminates.aspx>. [Accessed: 10- Jan- 2018].
- M. Zada and H. Yoo, "A miniaturized triple-band implantable antenna system for bio-telemetry applications," *IEEE Transactions on Antennas and Propagation*, vol. 66, no. 12, pp. 7378–7382, Dec. 2018.
- S. A. A. Shah and H. Yoo, "Scalp-Implantable Antenna Systems for Intracranial Pressure Monitoring," *IEEE Transactions on Antennas and Propagation*, vol. 66, no. 4, pp. 2170–2173, Aprl. 2018.
- F. Faisal and H. Yoo, "A miniaturized novel-shape dual-band antenna for implantable applications," *IEEE Transactions on Antennas and Propagation*, vol. 67, no. 2, pp. 774–783, Feb. 2019.